Irreversible Structural Transitions in Mixed Micelles of Oppositely Charged Diblock Copolymers in Aqueous Solution

Ilja K. Voets,* Arie de Keizer, and Martien A. Cohen Stuart

Laboratory of Physical Chemistry and Colloid Science, Wageningen University, Dreijenplein 6, 6703 HB Wageningen, The Netherlands

Justyna Justynska and Helmut Schlaad

Max Planck Institute of Colloids and Interfaces, Colloid Department, Research Campus Golm, 14424 Potsdam, Germany

Received June 27, 2006; Revised Manuscript Received January 5, 2007

ABSTRACT: Using light scattering (titration) measurements, we have shown that micelles can be formed in aqueous solutions of a mixture of poly(4-(2-amino hydrochloride-ethylthio)butylene)-*block*-poly(ethylene oxide), $PAETB_{49}$-*b*-PEO_{212}, and poly(4-(2-sodium carboxylate-ethylthio)butylene)-*block*-poly(ethylene oxide), $PCETB_{47}$-*b*-PEO_{212}. The driving force is not only electrostatic attraction between the oppositely charged polyelectrolyte blocks, but also hydrophobic interaction contributes. For pH < 5.3 or pH > 9.7 the single acid or alkaline diblock copolymer also forms micelles due to absence of electrostatic repulsion and the presence of only hydrophobic interaction. The mixed micelles formed under so-called optimal conditions (pH = 7.2, 10 mM $NaNO_3$, $T = 25.0$ °C) irreversibly shrink upon an increase in pH, ionic strength, and temperature and upon a decrease in pH. Restoring pH or temperature to the critical value has no effect on the hydrodynamic radius. We propose to relate these changes to an irreversible transition of the micellar core from a metastable fluidlike state (complex coacervate like) to a more stable glasslike state, triggered by a shift in the balance between electrostatic and hydrophobic interactions.

Introduction

When two aqueous solutions of oppositely charged diblock copolymers are mixed, complex coacervate core micelles (C3Ms),[1−3] also known as polyion complex micelles,[4−7] block ionomer complex micelles,[8,9] or interpolyelectrolyte complexes (IPEC),[10] may form depending on pH, ionic strength, and mixing fraction f_+. We define f_+ as the number of positively chargeable monomers divided by the total number of chargeable monomers.

$$f_+ = \frac{[n_+]}{[n_+] + [n_-]} \tag{1}$$

Characteristic features of these types of micelles[8,10−12] are their reversible and responsive nature. C3Ms dissociate above a critical ionic strength due to charge screening. Micelles formed from polymers containing a weak polyelectrolyte block dissociate below and/or above a critical pH, where one of the blocks has too low a charge density. Indeed, the micelles only exist in a narrow region around charge neutrality or charge stoichiometry, such that they do not exist below and above a critical f_+. Furthermore, the steady state is independent of the method of preparation. For example, the same structures are obtained in solution when a solution of the positive diblock copolymer (dbp^+) is titrated into a solution of the negative diblock copolymer (dbp^-) and vice versa. Hence, C3Ms seem to be in thermodynamic equilibrium: they form spontaneously and reversibly and are responsive to external stimuli, such as pH and ionic strength.

On the contrary, in the case of traditional polymeric micelles, consisting of one amphiphilic polymer, a state of thermodynamic equilibrium is generally not reached within experimental time scales. Particularly when the water-insoluble, core-forming component has a high glass temperature (as for example polystyrene) so-called "frozen" structures are formed.[12−14]

In this study we have investigated a mixture of two block copolymers (poly(4-(2-amino hydrochloride-ethylthio)butylene)-*block*-poly(ethylene oxide), $PAETB_{49}$-*b*-PEO_{212}, and poly(4-(2-sodium carboxylate-ethylthio)butylene)-*block*-poly(ethylene oxide), $PCETB_{47}$-*b*-PEO_{212}), of which the individual polymers can form this latter type of polymeric micelles with a hydrophobic core. Upon mixing aqueous solutions of positively charged $PAETB_{49}$-*b*-PEO_{212} and negatively charged $PCETB_{47}$-*b*-PEO_{212}, mixed micelles are formed with features characteristic of C3Ms as long as experimental conditions are within certain boundaries. When these are crossed, the C3Ms undergo a structural transition toward another type of mixed micelle that is smaller, contains less water in its core, and is hardly responsive to its environment. Very similar transitions have been reported on a solid−liquid interface[15−17] (polyelectrolyte multilayers) and on a liquid−liquid interface[18−21] (polyelectrolyte multilayer capsules), where it is argued that intercalated water is expelled from the polyelectrolyte multilayer during the transition triggered by heating or compression. Hence, we report on mixed micelles with tunable responsiveness by careful control over the experimental parameters.

The potential of C3Ms in a variety of applications, including the encapsulation of proteins, DNA, dendrimers, and drugs as well as hydrophobic and hydrophilic (charged and neutral) colloids,[3] spans a wide variety of disciplines ranging from medical implants and foodstuff encapsulation to personal care products and membrane filtration systems. The micelles described in this paper have additional advantages: enhanced stability and tunable responsiveness. In the field of drug delivery and controlled release, the major drawback of C3Ms' responsive

* Corresponding author. E-mail: ilja.voets@wur.nl.

10.1021/ma0614444 CCC: $37.00
Published on Web 02/22/2007

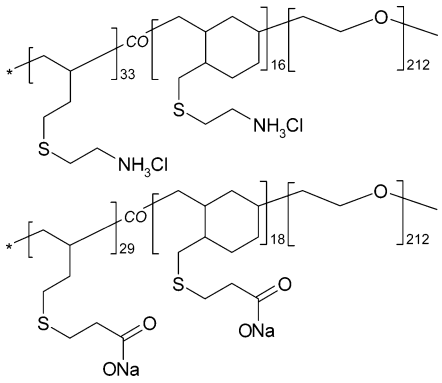

Figure 1. Chemical structure of the diblock copolymers used in this study. Poly(4-(2-amino hydrochloride-ethylthio)butylene)-*block*-poly(ethylene oxide), $PAETB_{49}$-*b*-PEO_{212} (top), and poly(4-(2-sodium carboxylate-ethylthio)butylene)-*block*-poly(ethylene oxide), $PCETB_{47}$-*b*-PEO_{212} (bottom).[28] The numbers beside the brackets denote the degree of polymerization.

nature is their relative instability which may potentially cause premature drug release as the micelles may dissociate in the bloodstream before reaching their target.[9,22−24] Instead of cross-linking of the micellar core or corona,[25,26] one may use polymers with a more hydrophobic backbone to circumvent dissociation. This approach may also be applied to coatings of adsorbed C3Ms, which have been shown to render a surface antifouling.[3] As C3Ms adsorb to a wide variety of surfaces (hydrophilic/hydrophobic, homogeneous/heterogeneous), simply by bringing the surface into contact with the C3M solution, preventing desorption of such a layer would be a great advantage in applications such as medical implants or membrane filters with respect to lifetime, cost, and, in the case of the former, cytotoxicity.

Experimental Part

Materials. Synthesis and characterization of the polymers used in this study have already been described elsewhere[27,28] (samples **G2** and **G3** in ref 28). The chemical structures are depicted in Figure 1.

Aqueous solutions of the polymers were prepared by dissolution of known amounts of polymer into deionized water (Milli-Q) to which known amounts of $NaNO_3$ were added, followed by a pH adjustment using NaOH and HNO_3. Unless otherwise specified, all experiments were performed at 25.0 °C at least 3 h after mixing polymer stock solutions of pH = 7.2 and 10 mM $NaNO_3$.

Dynamic and Static Light Scattering. Light scattering measurements were performed on an ALV light scattering instrument equipped with an ALV-5000 digital correlator and a 400 mW argon ion laser operated at a wavelength of 514.5 nm. A refractive index matching bath of filtered *cis*-decalin surrounded the cylindrical scattering cell, and the temperature was controlled at 25 ± 0.1 °C using a Haake C35 thermostat.

Light scattering titrations (LS-T) were carried out using a Schott-Geräte computer-controlled titration setup to control sequential addition of titrant and cell stirring. The pH was measured with a combined Ag/AgCl glass electrode. These values were converted into pH values after calibration of the electrode. During the mole fraction titrations (Figure 7), $PCETB_{47}$-*b*-PEO_{212} is titrated with a concentrated solution of $PAETB_{49}$-*b*-PEO_{212}. Typical concentrations of the titrated species are in the order of several mmol L^{-1}, expressed in terms of monomer concentration. During the salt and pH titrations, a $NaNO_3$ solution (salt LS-T, Figure 5) or NaOH and HNO_3 solutions (pH LS-T, Figure 2) were added to a solution of $PAETB_{49}$-*b*-PEO_{212} and $PCETB_{47}$-*b*-PEO_{212} under optimal conditions (pH = 7.2, 10 mM $NaNO_3$, T = 25.0 °C). After every dosage, pH, 90° light scattering intensity ($I_{90°}$), and the second-order correlation function $G_2(t)$ were recorded, the latter two 5 times during 20−25 s. Consecutively, the five values of $I_{90°}$ and $R_{h,90°}$ (method of cumulants, see below) were averaged, as well as the five second-order correlation functions prior to CONTIN analysis; i.e., CONTIN analysis (see below) was performed on the averaged $G_2(t)$. Data were reported in terms of total scattered intensity normalized to total polymer weight concentration ($I_{90°}/C_p$) and apparent hydrodynamic radius ($R_{h,90°}$) as a function of pH, f_+, and ionic strength. LS-T measurements have primarily been analyzed according to the method of cumulants[29] using the standard ALV software. A more detailed analysis has been performed by fitting $G_2(t)$ with the Provencher program CONTIN.[30,31] Note that all values of $R_{h,90°}$ reported in this paper are apparent values, since no extrapolation to $q = 0$ has been performed. Moreover, where scattering intensity is low (for example, regime III in Figure 2a,b) sampling time could be increased to obtain more reliable values of $R_{h,90°}$.

Cryogenic Transmission Electron Microscopy (Cryo-TEM). Cryo-TEM observations were carried out with a Technai Sphera (FEI Co.) transmission electron microscope operating at a voltage of 120 kV. Samples were prepared on 200 mesh copper grids containing a carbon-coated holey support film (Agar Scientific, UK, and Ted Pella Inc., USA). A small drop of sample was placed on the specimen grid, and the excess fluid was blotted off using Whatmann #4 filter paper. Preparation was carried out in an environmental chamber with high relative humidity to prevent drying and subsequent precooling of the dispersions. The thin aqueous films were vitrified in melting ethane and transferred under liquid nitrogen into a Gatan CT3500 cryo holder and subsequently into the transmission electron microscope. Images were taken under low dose conditions.

Results and Discussion

Effect of pH. $R_{h,90°}$ and $I_{90°}/C_p$ are plotted as a function of pH for $PAETB_{49}$-*b*-PEO_{212} (Figure 2a), $PCETB_{47}$-*b*-PEO_{212} (Figure 2b), and their 1:1 mixture (Figure 2c,d). In Figure 2a, we clearly observe three regimes. In regime I (pH > 9.7), we observe a high scattering intensity and $R_{h,90°} = 17.9 \pm 0.6$ nm, whereas in regime III (pH < 8.7) the scattering intensity is low and $R_{h,90°} = 97 \pm 17$ nm. A similar picture can be seen in Figure 2b, where regime I (pH < 5.3) corresponds to high scattering intensity and a $R_{h,90°} = 14.9 \pm 0.5$ nm, while in regime III (pH > 6.2) the scattering intensity is low and $R_{h,90°}$ is high ($R_{h,90°} = 129 \pm 31$ nm, values are rather scattered).

Regime I corresponds to the pH region where micelles are formed with a core consisting of water-insoluble, uncharged PAETB-blocks (high pH, Figure 2a) and PCETB-blocks (low pH, Figure 2b) stabilized by a PEO corona. The micellization is reversible, as one can repeatedly increase and decrease the pH resulting in a cycle of association and dissociation of the micelles (data not shown). Regime III corresponds to a regime without micelles.

CONTIN analysis of $G_2(t)$ for $PAETB_{49}$-*b*-PEO_{212} (Figure 3a) and $PCETB_{47}$-*b*-PEO_{212} (Figure 3b) confirms this pH-dependent micellization. In Figure 3a, we observe two modes for all pH values. The position of the fast mode is pH independent in regimes I and III but shifts in the transition region from $R_{h,90°} = 3 \pm 1$ nm (regime III) to $R_{h,90°} = 12.4 \pm 0.4$ nm (regime I). The position of the slow mode ($R_{h,90°} = 106 \pm 22$ nm, values are rather scattered) is pH independent, while its amplitude decreases slightly with increasing pH. In Figure 3b, we observe a transition from two modes in the CONTIN profile for pH > 6.2 (regime III) to a nearly single mode for pH < 5.3 (regime I). As in Figure 3a, the position of the slow mode ($R_{h,90°} = 108 \pm 17$ nm, values are rather scattered) is nearly pH independent, but now its amplitude decreases considerably with decreasing pH. The position of the fast mode is pH independent in regimes I and III but shifts in the transition region from $R_{h,90°}$

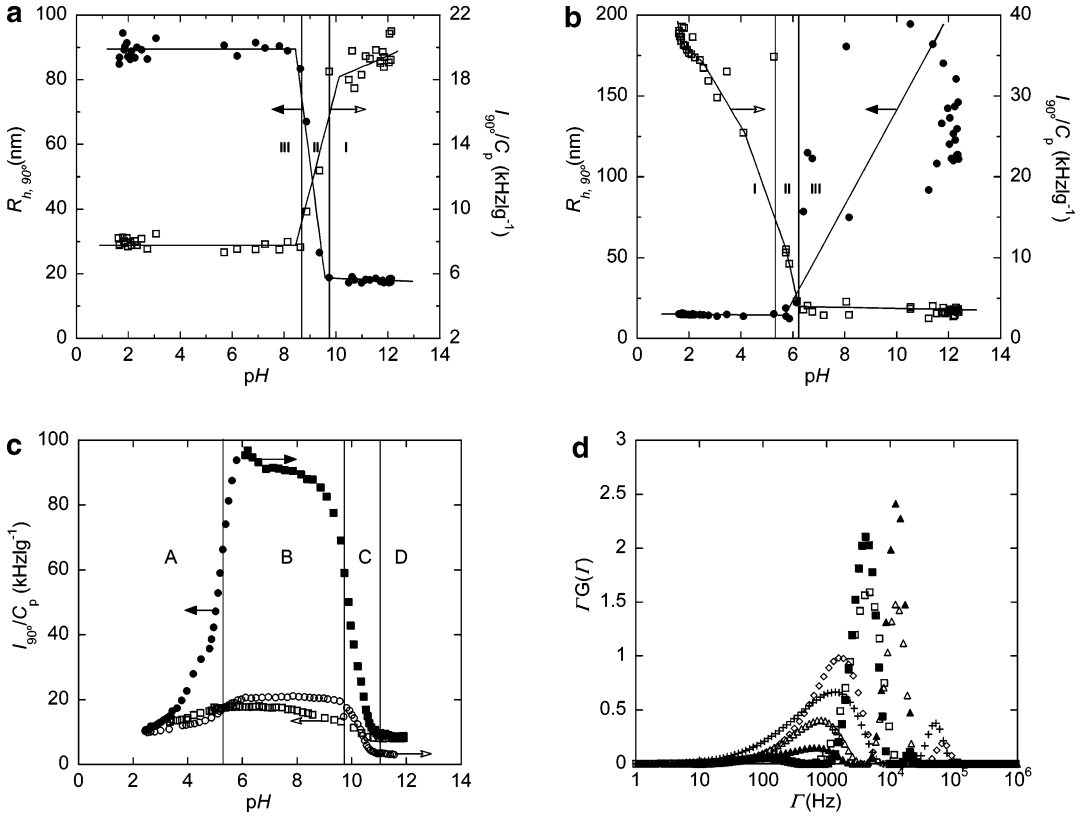

Figure 2. (a) $R_{h,90°}$ (closed circles) and $I_{90°}/C_p$ (open squares) as a function of pH for an aqueous solution of $PAETB_{49}$-*b*-PEO_{212} at 10 mM $NaNO_3$, $C_p = 2.55-1.46$ g L^{-1} and 25.0 °C. A line is drawn through the data points as a guide to the eye. Arrows indicate corresponding axes. (b) $R_{h,90°}$ (closed circles) and $I_{90°}/C_p$ (open squares) as a function of pH for an aqueous solution of $PCETB_{47}$-*b*-PEO_{212} at 10 mM $NaNO_3$, $C_p = 0.99-0.64$ g L^{-1} and 25.0 °C. A line is drawn through the data points as a guide to the eye. Arrows indicate corresponding axes. (c) $I_{90°}/C_p$ as a function of pH for an aqueous solution of $PAETB_{49}$-*b*-PEO_{212} and $PCETB_{47}$-*b*-PEO_{212} at 10 mM $NaNO_3$, $C_p = 1.95-1.39$ g L^{-1}, $f_+ = 0.491$, and 25.0 °C. The arrows indicate the direction of the pH scan. The filled symbols correspond to the first pH scan (circles: first scan down; squares: first scan up), and the open symbols correspond to the second (consecutive) pH scan. The lines mark regions A−D (A: 2.5 < pH < 5.3; B: 5.3 < pH < 9.7; C: 9.7 < pH < 11; D: 11 < pH < 12). (d) CONTIN distribution as a function of pH for an aqueous solution of $PAETB_{49}$-*b*-PEO_{212} (◇: pH = 7.8), $PCETB_{47}$-*b*-PEO_{212} (+: pH = 8.2), and their 1:1 mixture (□: pH = 8.4, pH increase in first scan; ■: pH = 5.8, pH decrease in first scan; △: pH = 8.0, pH decrease in second scan; ▲: pH = 8.4, pH increase in second scan) at 10 mM $NaNO_3$, $C_p = 1.95-1.39$ g L^{-1}, and 25.0 °C.

$= 2 \pm 1$ nm (regime III) to $R_{h,90°} = 13.1 \pm 0.6$ nm (regime I). The values of $R_{h,90°}$ determined by the methods of cumulants and CONTIN agree quite well. $R_{h,90°,CUM}$ is slightly larger than $R_{h,90°,CONTIN}$ (fast mode) due to the presence of the second slow mode.

The q^2-dependent fast mode in CONTIN (see Supporting Information) corresponds to the diffusion of micelles in regime I and polymers in regime III. The q^2-dependent slow mode (see Supporting Information) that dominates the CONTIN profile in regime III, which causes large values of R_h in the cumulant method, corresponds to a small number of aggregates and/or very large but loose aggregates (i.e., low polymer density). Upon filtration of the solutions in regime III over a 0.2 μm filter, $I_{90°}$ decreases considerably (75% for $PAETB_{49}$-*b*-PEO_{212} and 64% for $PCETB_{47}$-*b*-PEO_{212}), while $I_{90°}$ is much less affected by filtration in regime I (9% for $PAETB_{49}$-*b*-PEO_{212} and 4% for $PCETB_{47}$-*b*-PEO_{212}), where the slow mode is much less dominant, i.e. nearly absent. These findings are in line with others by for example Gohy et al.,[32] who observed aggregates for P2VP−PDMAEMA at pH < 4.5 in a regime of low scattering intensity and large hydrodynamic radius.

Figure 2c shows that the effect of pH on the 1:1 mixture is clearly different from its effect on the separate polymers. Upon mixing aqueous solutions of $PAETB_{49}$-*b*-PEO_{212} and $PCETB_{47}$-*b*-PEO_{212} at pH = 7.2 rather large micelles are formed that scatter light considerably ($R_{h,90°} = 32.3 \pm 0.6$ nm, cumulant analysis; $R_{h,90°} = 31.0 \pm 1.7$ nm, CONTIN analysis; $I_{90°} > 170$ kHz). Upon pH increase (or pH decrease), these aggregates shrink ($R_{h,90°} = 15.1 \pm 0.4$ nm, cumulant analysis; $R_{h,90°} = 11.0 \pm 0.6$ nm, CONTIN analysis; $I_{90°} < 40$ kHz) to a size comparable to and slightly smaller than the $R_{h,90°}$ of the micelles consisting of either $PCETB_{47}$-*b*-PEO_{212} or $PAETB_{49}$-*b*-PEO_{212} respectively. When pH is decreased (or increased) to the initial value, the initial state is not regained, i.e., $R_{h,90°} \neq 31-32$ nm. Instead, $R_{h,90°}$ and $I_{90°}$ remain practically independent of pH in the whole pH regime for 2.5 < pH < 12. In the intermediate pH regime, 6.2 < pH < 8.7 the micelles are necessarily mixed micelles, as no micelles exist in the single polymer solutions. CONTIN analysis (Figure 2d) confirms that the objects found in the mixture of $PAETB_{49}$-*b*-PEO_{212} and $PCETB_{47}$-*b*-PEO_{212} for 6.2 < pH < 8.7 are not observed in the solutions of either $PAETB_{49}$-*b*-PEO_{212} or $PCETB_{47}$-*b*-PEO_{212}.

Upon closer inspection of $I_{90°}$ and $R_{h,90°}$ vs pH (Figure 2c,d) in combination with a CONTIN analysis at different pH values after the initial decrease in $I_{90°}$ and $R_{h,90°}$ (after first pH titration run), we observe subtle changes in both parameters. We can identify four regions, A−D (Figure 2c). As discussed above, for intermediate pH values (region B: 5.3 < pH < 9.7) we observe nearly constant $I_{90°}$ and $R_{h,90°}$ corresponding to mixed micelles. Outside this region B, micelles are observed in solutions of either diblock copolymers. Thus, one might expect to observe micelles of $PAETB_{49}$-*b*-PEO_{212} and unimerically dissolved $PCETB_{47}$-*b*-PEO_{212} in regions C and D (pH > 9.7) and vice versa in region A (pH < 5.3), i.e., the dissociation of

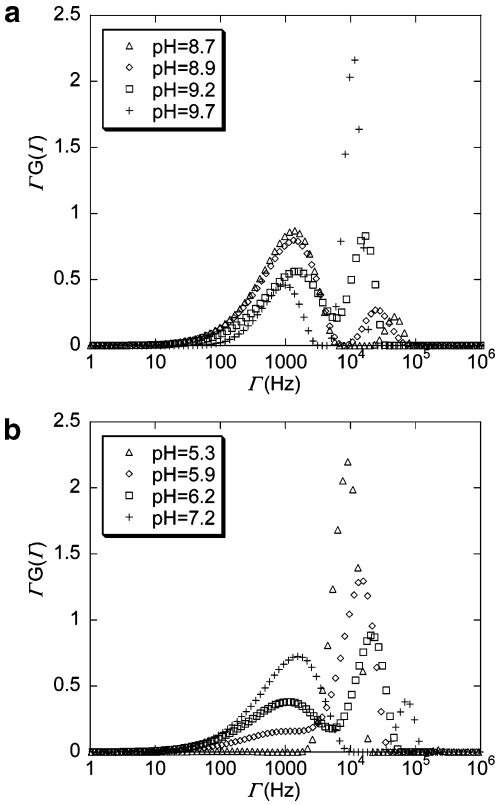

Figure 3. (a) CONTIN distribution as a function of pH (△: pH = 8.7; ◇: pH = 8.9; □: pH = 9.2, +: pH = 9.7) for an aqueous solution of $PAETB_{49}$-*b*-PEO_{212} at 10 mM $NaNO_3$, $C_p = 2.55-1.46$ g L^{-1}, and 25.0 °C. (b) CONTIN distribution as a function of pH (△: pH = 5.3; ◇: pH = 5.9; □: pH = 6.2, +: pH = 7.2) for an aqueous solution of $PCETB_{47}$-*b*-PEO_{212} at 10 mM $NaNO_3$, $C_p = 0.99-0.64$ g L^{-1}, and 25.0 °C.

mixed micelles above and below pH_{cr}, respectively, as typically observed for C3Ms. In fact, we observe a decrease in $I_{90°}$ and $R_{h,90°,CONTIN}$ in region C ($9.7 < pH < 11$), resulting in a low $I_{90°}$ and $R_{h,90°,CONTIN}$ (but large $R_{h,90°,CUM}$ due to the dominant contribution of a slow mode; compare regime III in Figure 2a,b) in region D ($11 < pH < 12$), which is consistent with a dissocation of the mixed micelles. However, we do not observe three peaks corresponding to a slow mode (those of $PCETB_{47}$-*b*-PEO_{212} and $PAETB_{49}$-*b*-PEO_{212} superimpose) and two diffusive modes, the $PAETB_{49}$-*b*-PEO_{212} micelles and $PCETB_{47}$-*b*-PEO_{212} polymers. Rather, we observe one slow mode and a diffusive mode with a $R_{h,90°} = 4.3 \pm 0.3$ nm. The data in region A ($2.5 < pH < 5.3$) seem more consistent with a decrease in size of the mixed micelles than with their dissociation. As in region D, we observe 2 not 3 peaks, corresponding to a slow mode and a fast diffusive mode with a $R_{h,90°}$ decreasing to a minimum of about 9 nm.

Clearly, the behavior of the mixture of $PCETB_{47}$-*b*-PEO_{212} and $PAETB_{49}$-*b*-PEO_{212} differs not only from the behavior of the individual polymers, it is also very different from the behavior of typical C3Ms (consisting of weak polyelectrolyte blocks) that dissociate reversibly above *and* below a critical pH,[12,33] as discussed in the Introduction. Apparently, the micellization in aqueous solutions of $PAETB_{49}$-*b*-PEO_{212} and $PCETB_{47}$-*b*-PEO_{212} is not reversible, as is the micellization of C3Ms and either $PAETB_{49}$-*b*-PEO_{212} or $PCETB_{47}$-*b*-PEO_{212}. We propose that this novel behavior originates from the segment chemistry of the polymers used in this study. $PAETB_{49}$-*b*-PEO_{212} and $PCETB_{47}$-*b*-PEO_{212} are block copolymers with a polyelectrolyte block that contains titratable groups covalently linked

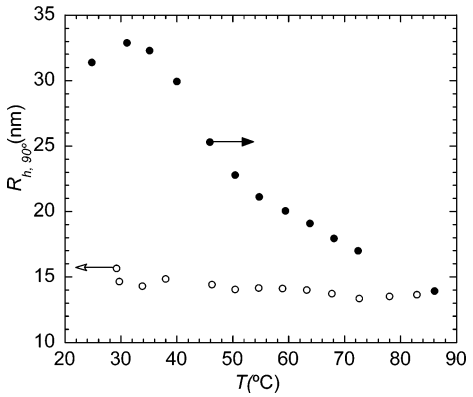

Figure 4. $R_{h,90°}$ as a function of temperature for a mixture of $PAETB_{49}$-*b*-PEO_{212} and $PCETB_{47}$-*b*-PEO_{212} (circles) at pH = 7.2, 10 mM $NaNO_3$, and $C_p = 1.77$ g L^{-1}, and $f_+ = 0.490$. The arrows indicate the direction of the temperature scan; the filled symbols correspond to the scan up, and the open symbols indicate the scan down.

to a rather hydrophobic backbone. Therefore, micellization occurs in aqueous solutions of the separate polymers, and hydrophobic interactions play a role in the formation of mixed micelles from aqueous solutions of $PAETB_{49}$-*b*-PEO_{212} and $PCETB_{47}$-*b*-PEO_{21}. In the intermediate pH regime, both electrostatic and hydrophobic interactions act as a driving force for micellization. Under these conditions, the behavior resembles that of C3Ms. When pH is sufficiently increased (or decreased) so that one of the polymers becomes effectively uncharged (i.e., micellization occurs in single-component solutions), the influence of the hydrophobic backbone becomes apparent, resulting in behavior that is strikingly different from "C3M behavior". Electrostatic interactions have confined the polymers in the intermediate pH regime within the same aggregate, but now hydrophobic interactions are increasingly more dominating and result in the expulsion of water from the micellar core: the micelles shrink. Apparently, hydrophobic interactions are strong enough to prevent the mixed micelles from dissociation in a regime of low charge density, at least for low pH values, where "normal" C3Ms would no longer exist.

Effect of Temperature. To test the reasoning above, we studied the effect of temperature (T) on the mixed micelles. The $R_{h,90°}$ of C3Ms is nearly independent of temperature,[33] as temperature essentially does not effect electrostatic interaction. On the contrary, hydrophobic interaction is temperature dependent.[34]

Figure 4 shows $R_{h,90°}$ for the 1:1 mixture as a function of temperature. Again, we clearly observe a shrinkage of the size of the mixed micelles: $R_{h,90°}$ decreases with increasing temperature from $R_{h,90°} = 31.6 \pm 0.3$ nm (cumulant analysis; $T = 24.9 \pm 0.1$ °C) to $R_{h,90°} = 14.2 \pm 0.2$ nm (cumulant analysis; $T = 87.0 \pm 0.2$ °C), while $I_{90°}$ decreases from $I_{90°} = 181.3 \pm 1.3$ kHz to $I_{90°} = 58.3 \pm 0.6$ kHz.

As was the case with pH, the initial state is not regained (i.e., $R_{h,90°}$ equal to about 32 nm) by restoring the temperature to its initial value. Instead, $R_{h,90°}$ and $I_{90°}$ remain practically independent of temperature after the initial response ($R_{h,90°} = 14.7 \pm 1.0$ nm and $I_{90°} = 51.8 \pm 2.4$ kHz for first down, second up, and second down scan, of which the latter two are not shown for clarity). This confirms the proposed idea that hydrophobic interactions are important in mixed micelles of $PAETB_{49}$-*b*-PEO_{212} and $PCETB_{47}$-*b*-PEO_{212}. Both pH and temperature can shift the balance between the hydrophobic and electrostatic driving forces for micellization, triggering a transition from a relatively hydrophilic, swollen state of the core into a more

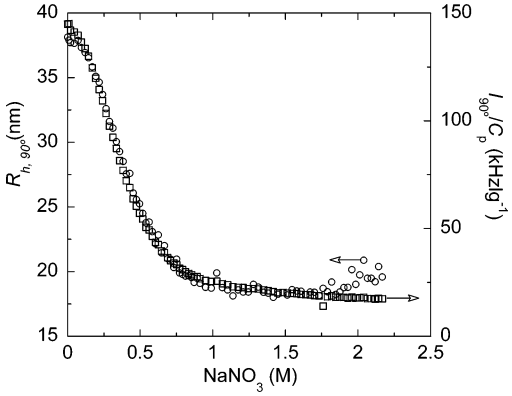

Figure 5. $R_{h,90°}$ (open circles) and $I_{90°}/C_p$ (open squares) as a function of the concentration added salt for the mixture of PAETB$_{49}$-*b*-PEO$_{212}$ and PCETB$_{47}$-*b*-PEO$_{212}$ at pH = 7.2, C_p = 0.90−0.64 g L^{-1}, f_+ = 0.490, and T = 25.0 °C. Arrows indicate corresponding axes.

hydrophobic, compact state. As the transition is irreversible, the initial state is probably metastable.

Effect of Ionic Strength. Naturally, parameters such as ionic strength and mixing fraction also influence the balance between electrostatic and hydrophobic driving forces. An increase in ionic strength, increases the charge screening, shifting the balance toward hydrophobic interaction. Thus, we expect to observe a decrease of $R_{h,90°}$ and $I_{90°}/C_p$ with increasing ionic strength.

$R_{h,90°}$ and $I_{90°}/C_p$ are plotted as a function of the concentration of added salt for a 1:1 mixture of PAETB$_{49}$-*b*-PEO$_{212}$ and PCETB$_{47}$-*b*-PEO$_{212}$ (Figure 5). As expected, $R_{h,90°}$ and $I_{90°}/C_p$ decrease with increasing ionic strength from $R_{h,90°}$ = 38.2 ± 0.2 nm (cumulant analysis; 0 mM added NaNO$_3$) to $R_{h,90°}$ = 18.8 ± 0.7 nm (cumulant analysis; [NaNO$_3$] > 950 mM) and $I_{90°}/C_p$ = 131.0 ± 0.5 kHz L g^{-1} to $I_{90°}/C_p$ = 20.0 ± 2.7 kHz L g^{-1}. Note that mixed micelles still exist at added salt concentrations as high as 2 M; i.e., they do not dissociate in the experimental range studied. This is in sharp contrast with the behavior observed for C3Ms that dissociate above typically 0.05−0.5 M added salt.[12,33] As described above for the effect of pH, hydrophobic interaction is apparently sufficient to stabilize the micelles under conditions where "normal" C3Ms would dissociate. The micellar core becomes considerably more hydrophobic with increasing ionic strength, expelling water, and consequently the hydrodynamic radius decreases. We have extended our scattering study with electron microscopy experiments, which are sensitive to differences in the transmission of electrons and therefore in principle to densification (due to increased hydrophobicity) of the micellar core.

Figure 6 shows electron micrographs of aqueous solutions of a 1:1 mixture of PAETB$_{49}$-*b*-PEO$_{212}$ and PCETB$_{47}$-*b*-PEO$_{212}$ before (Figure 6a) and after a temperature scan (Figure 6b). The micelles appear as gray spots in Figure 6a and darker gray spots in Figure 6b, which is consistent with a denser micellar core after the temperature scan.

Effect of Mixing Fraction. Interestingly, the effect of f_+ on aqueous solutions containing both PAETB$_{49}$-*b*-PEO$_{212}$ and PCETB$_{47}$-*b*-PEO$_{212}$ is slightly more complex and can be divided into two categories depending on the pH of the stock solutions. $I_{90°}/C_p$ is plotted as a function of f_+ for different pH values (Figure 7a). Two regimes of initial pH can be distinguished: in regime I (5.4 < pH < 6.0), $I_{90°}/C_p$ increases monotonically for f_+ < PMC (wherein PMC is the so-called preferred micellar concentration[2]), while $I_{90°}/C_p$ decreases with a single slope for f_+ > PMC. In regime II (6.9 < pH < 7.2), two regions with different slopes can be distinguished for f_+ < PMC and f_+ > PMC. In the regions closest to the PMC, the curves of $R_{h,90°}$ and $I_{90°}/C_p$ vs f_+ follow the same trend (Figure 7c). This behavior is not observed in regime I: there are no values of f_+ where the curves of $R_{h,90°}$ and $I_{90°}/C_p$ are congruent (Figure 7b).

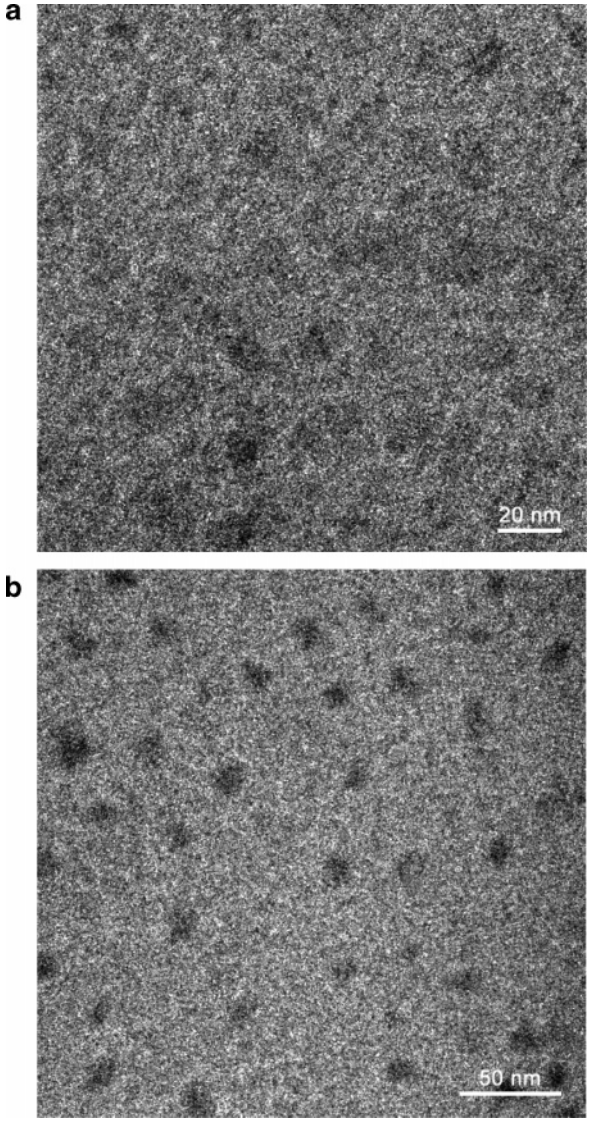

Figure 6. (a) Cryo-TEM image of a solution of a mixture of PAETB$_{49}$-*b*-PEO$_{212}$ and PCETB$_{47}$-*b*-PEO$_{212}$ (pH = 7.2, 10 mM NaNO$_3$, C_p = 1.85 g L^{-1}, f_+ = 0.491, and T = 25.0 °C). (b) Cryo-TEM image of a solution of a mixture of PAETB$_{49}$-*b*-PEO$_{212}$ and PCETB$_{47}$-*b*-PEO$_{212}$ after the temperature scan shown in Figure 4 (pH = 7.2, 10 mM NaNO$_3$, C_p = 1.77 g L^{-1}, f_+ = 0.490, and T = 25.0 °C).

It is likely that in the mixtures of regime I no mixed micelles are formed. The pH of the polymer stock solutions is in the vicinity of the critical pH for formation of micelles of PCETB$_{47}$-*b*-PEO$_{212}$ alone (pH$_c$ = 5.3). As the pH is not buffered during a light scattering titration, it will change due to changes in the degree of dissociation of the PAETB and PCETB blocks of the diblock copolymers due to complexation.[2] In regime I, pH decreases with increasing f_+ for f_+ < PMC until PMC is reached (data not shown), while for f_+ > PMC pH is nearly constant at a value of ∼3.2 (initial pH = 5.4/6.0, respectively). Thus, for f_+ < PMC PCETB$_{47}$-*b*-PEO$_{212}$ alone forms more and more micelles with increasing f_+ (as pH decreases), resulting in a monotonous increase in $I_{90°}/C_p$, resembling the increase in intensity with decreasing pH in Figure 2b in the same pH range. For f_+ > PMC, pH remains nearly constant, resulting in a nearly constant number of micelles. However, the number of free PAETB$_{49}$-*b*-PEO$_{212}$ polymers increases (as f_+ increases), while

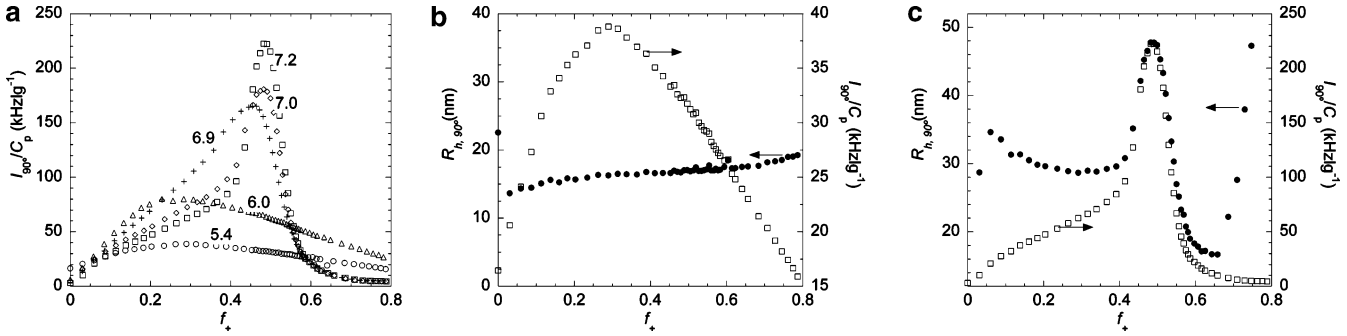

Figure 7. (a) $I_{90°}/C_p$ as a function of mixing fraction for the mixture of $PAETB_{49}$-*b*-PEO_{212} and $PCETB_{47}$-*b*-PEO_{212} at 10 mM $NaNO_3$, C_p = 0.99−3.42 g L^{-1}, 25.0 °C, and various pH (○: pH = 5.4; △: pH = 6.0; +: pH = 6.9; ◇: pH = 7.0; □: pH = 7.2). (b) $R_{h,90°}$ (closed circles) and $I_{90°}/C_p$ (open squares) as a function of mixing fraction for the mixture of $PAETB_{49}$-*b*-PEO_{212} and $PCETB_{47}$-*b*-PEO_{212} at 10 mM $NaNO_3$, C_p = 0.99−3.41 g L^{-1}, 25.0 °C, and pH = 5.4. Arrows indicate corresponding axes. (c) $R_{h,90°}$ (closed circles) and $I_{90°}/C_p$ (open squares) as a function of mixing fraction for the mixture of $PAETB_{49}$-*b*-PEO_{212} and $PCETB_{47}$-*b*-PEO_{212} at 10 mM $NaNO_3$, C_p = 0.99−3.42 g L^{-1}, 25.0 °C, and pH = 7.2. Arrows indicate corresponding axes.

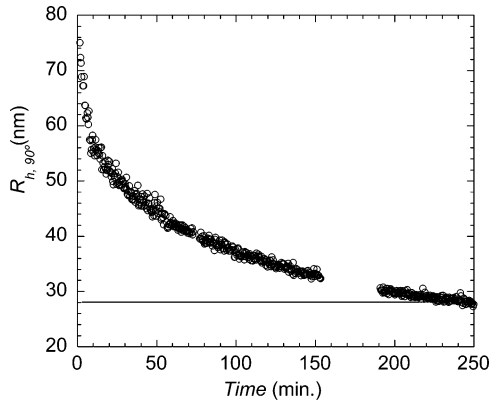

Figure 8. $R_{h,90°}$ as a function of time for a mixture of $PAETB_{49}$-*b*-PEO_{212} and $PCETB_{47}$-*b*-PEO_{212} (○) at pH = 7.2, 10 mM $NaNO_3$, C_p = 1.95 g L^{-1}, f_+ = 0.491, and T = 25.0 °C. The line indicates $R_{h,90°}$ = 28.0 nm, measured 3 days after preparation.

they contribute relatively little to $I_{90°}$, but equally to C_p, resulting in a decrease of $I_{90°}/C_p$ for f_+ > PMC.

In regime II, pH remains within the intermediate pH range, where no micelles are formed in solutions of either $PAETB_{49}$-*b*-PEO_{212} or $PCETB_{47}$-*b*-PEO_{212} (5.3 < pH < 9.6). Thus, both polymers are sufficiently charged to drive the formation of mixed micelles through electrostatic interaction. Therefore, we observe a difference in the effect of f_+ on $I_{90°}/C_p$ and $R_{h,\,90°}$, namely two regions with different slopes for both f_+ < PMC and f_+ > PMC, as has been described previously for fully reversible C3Ms.[2,11] Apparently, the formation of mixed micelles consisting of $PAETB_{49}$-*b*-PEO_{212} and $PCETB_{47}$-*b*-PEO_{212} is reversible with respect to f_+, as is the case for C3Ms in general.[2,12,33]

Effect of Time. Contrary to C3Ms, polymeric micelles with a hydrophobic core tend to relax so slowly that a state of thermodynamic equilibrium is generally not reached within experimental time scales. Thus, we investigated the effect of time on the size of the mixed micelles after preparation of the two polymer stock solutions (Figure 8). Indeed, we observe a decrease in micellar size in the first 4 h after preparation from $R_{h,90°}$ = 75 nm to $R_{h,90°}$ = 28.2 ± 0.5 nm. After 4 h, $R_{h,90°}$ has reached an almost constant value (i.e., $R_{h,90°}$ = 28.0 ± 0.9 nm, measured 3 days after preparation).

However, the effect of pH, ionic strength, and temperature on the micellar size is qualitatively independent of the period after preparation; i.e., the observed trends in $R_{h,90°}$ vs pH, ionic strength, and temperature as described above are also observed in solutions of $PAETB_{49}$-*b*-PEO_{212} and $PCETB_{47}$-*b*-PEO_{212} prepared several days before the experiments (data not shown).

Conclusions

Using light scattering measurements, we have shown that micelles can be formed in aqueous solutions of poly(4-(2-amino hydrochloride-ethylthio)butylene)-*block*-poly(ethylene oxide), $PAETB_{49}$-*b*-PEO_{212}, poly(4-(2-sodium carboxylate-ethylthio)-butylene)-*block*-poly(ethylene oxide), $PCETB_{47}$-*b*-PEO_{212}, and a mixture of the two.

In aqueous solutions of either $PAETB_{49}$-*b*-PEO_{212} or $PCETB_{47}$-*b*-PEO_{212}, micelles are formed when polymer charge density is low (pH < 5.3 for $PCETB_{47}$-*b*-PEO_{212} and pH > 9.7 for $PAETB_{49}$-*b*-PEO_{212}). Under these circumstances, the "polyelectrolyte" blocks are effectively water-insoluble, resulting in micelles due to hydrophobic interactions. In aqueous solutions of $PAETB_{49}$-*b*-PEO_{212} and $PCETB_{47}$-*b*-PEO_{212}, mixed micelles are formed. Two different states can be distinguished. The first state corresponding to a metastable mixed micelle with a swollen, gel-like core is reached immediately after mixing the separate polymer solutions at intermediate pH and f_+, low ionic strength, and moderate temperature. When these aggregates are "treated" by a considerable increase in pH, ionic strength, or temperature or by a decrease in pH, the second state is reached, corresponding to a more stable state with a glasslike micellar core.

The metastable state shows several similarities to "normal" C3Ms. First, for pH ≥ 6.9 the micelles dissociate upon under-/overdosing of $PAETB_{49}$-*b*-PEO_{212}. Second, the micelles are responsive to their environment. But there are also clear differences: these mixed micelles have enhanced stability as they are stable up to 2 M of $NaNO_3$ and in a wide pH region (2.5 < pH < 9.7), which are circumstances where C3Ms typically no longer exist. Furthermore, the hydrodynamic size of these aggregates is strongly dependent on temperature. Apparently, these micelles are not typical C3Ms, formed through electrostatic interaction only, but a combination of electrostatic and hydrophobic interactions drives their micellization.

The structural transition occurring upon pH, T, or ionic strength "treatment" into the second, more stable state is caused by a shift in the balance between the two driving forces. Hydrophobic interactions are favored in such a way that water is expelled from the core as it becomes increasingly more hydrophobic, while the micelles shrink about a factor of 2 in size. A similar phenomenon has been reported previously for polyelectrolyte multilayer systems on flat and curved surfaces.[15−21] As the initial state is metastable, the structural transition is

irreversible. Once the micelles have a glasslike core, they hardly respond to a change in environment. For example, after a pH or temperature treatment, the R_h is nearly fixed, irrespective of changes in pH or temperature.

We relate this novel behavior to the chemical properties of the polymer segments used in this study. $PAETB_{49}$-*b*-PEO_{212} and $PCETB_{47}$-*b*-PEO_{212} are block copolymers with a polyelectrolyte block that contains titratable groups covalently linked to a rather hydrophobic backbone. Therefore, micellization occurs in aqueous solutions of the separate species, and hydrophobic interactions play a role in the formation of mixed micelles when these aqueous solutions are mixed. Ion pairs in water have interaction energies of a few *kT*, whereas in a low dielectric cavity this energy may become of order 100 *kT*. Hence, a rather hydrophobic backbone resulting in a rather hydrophobic micellar core stabilizes the polyelectrolyte complexes enormously.

By carefully controlling the experimental parameters, one can tune the transition toward more stable and less responsive micelles. Hence, stability and responsiveness have become tunable parameters. Naturally, this will positively affect the applicability of these micelles in industrial and biomedical applications.

Acknowledgment. This work has been carried out in the framework of the EU Polyamphi/Marie Curie program (FP6-2002, proposal 505027). One of us was financed by the SONS Eurocores program (Project JA016-SONS-AMPHI). The authors gratefully thank Johan Hazekamp (Unilever, Vlaardingen), who performed the cryo-TEM measurements, as well as Remco Fokkink and Peter Barneveld for their technical support with the light scattering measurements and software, respectively (AfterALV, www.dullware.nl).

Supporting Information Available: DLS measurements as a function of scattering angle, θ, for $30° < \theta < 145°$. This material is available free of charge via the Internet at http://pubs.acs.org.

References and Notes

(1) Cohen Stuart, M. A.; Besseling, N. A. M.; Fokkink, R. G. *Langmuir* **1998**, *14*, 6846−6849.
(2) van der Burgh, S.; de Keizer, A.; Cohen, Stuart, M. A. *Langmuir* **2004**, *20*, 1073−1084.
(3) van der Burgh, S.; Fokkink, R.; de Keizer, A.; Cohen Stuart, M. A. *Colloids Surf., A* **2004**, *242*, 167−174.
(4) Harada, A.; Kataoka, K. *Macromolecules* **1995**, *28*, 5294−5299.
(5) Harada, A.; Kataoka, K. *J. Macromol. Sci., Part A: Pure Appl. Chem.* **1997**, *A34*, 2119−2133.
(6) Harada, A.; Kataoka, K. *Macromolecules* **1998**, *31*, 288−294.
(7) Harada, A.; Kataoka, K. *J. Am. Chem. Soc.* **1999**, *121*, 9241−9242.
(8) Kabanov, A. V.; Bronich, T. K.; Kabanov, V. A.; Yu, K.; Eisenberg, A. *Macromolecules* **1996**, *29*, 6797−6802.
(9) Kabanov, A. V.; Kabanov, V. A. *Adv. Drug Delivery Rev.* **1998**, *30*, 49−60.
(10) Gohy, J. F.; Varshney, S. K.; Jerome, R. *Macromolecules* **2001**, *34*, 3361−3366.
(11) van der Burgh, S. Complex Coacervate Core Micelles in Solution and at Interfaces. Ph.D. thesis, Wageningen Universiteit: Wageningen, 2004.
(12) Cohen Stuart, M. A.; Hofs, B.; Voets, I. K.; de Keizer, A. *Curr. Opin. Colloid Interface Sci.* **2005**, *10*, 30−36.
(13) Moffitt, M.; Khougaz, K.; Eisenberg, A. *Acc. Chem. Res.* **1996**, *29*, 95−102.
(14) Riess, G. *Prog. Polym. Sci.* **2003**, *28*, 1107−1170.
(15) Wang, B.; Feng, J.; Gao, C. *Colloids Surf., A* **2005**, *259*, 1−5.
(16) Gao, C. Y.; Wang, B.; Feng, J.; Shen, J. C. *Macromolecules* **2004**, *37*, 8836−8839.
(17) Lvov, Y.; Decher, G.; Möhwald, H. *Langmuir* **1993**, *9*, 481−486.
(18) Kohler, K.; Shchukin, D. G.; Sukhorukov, G. B.; Möhwald, H. *Macromolecules* **2004**, *37*, 9546−9550.
(19) Vinogradova, O. I. *J. Phys.: Condens. Matter* **2004**, *16*, R1105−R1134.
(20) Fery, A.; Dubreuil, F.; Möhwald, H. *New J. Phys.* **2004**, *6*.
(21) Gao, C. Y.; Leporatti, S.; Moya, S.; Donath, E.; Möhwald, H. *Chem.−Eur. J.* **2003**, *9*, 915−920.
(22) Jones, M. C.; Leroux, J. C. *Eur. J. Pharmacol. Biopharm.* **1999**, *48*, 101−111.
(23) Kakizawa, Y.; Kataoka, K. *Adv. Drug Delivery Rev.* **2002**, *54*, 203−222.
(24) Kataoka, K.; Harada, A.; Nagasaki, Y. *Adv. Drug Delivery Rev.* **2001**, *47*, 113−131.
(25) Jaturanpinyo, M.; Harada, A.; Yuan, X. F.; Kataoka, K. *Bioconjugate Chem.* **2004**, *15*, 344−348.
(26) Miyata, K.; Kakizawa, Y.; Nishiyama, N.; Harada, A.; Yamasaki, Y.; Koyama, H.; Kataoka, K. *J. Am. Chem. Soc.* **2004**, *126*, 2355−2361.
(27) Justynska, J.; Schlaad, H. *Macromol. Rapid Commun.* **2004**, *25*, 1478−1481.
(28) Justynska, J.; Hordyjewicz, Z.; Schlaad, H. *Polymer* **2005**, *46*, 12057−12064.
(29) Koppel, D. E. *J. Chem. Phys.* **1972**, *57*, 4814−4820.
(30) Provencher, S. W. *Comput. Phys. Commun.* **1982**, *27*, 213−227.
(31) Provencher, S. W. *Comput. Phys. Commun.* **1982**, *27*, 229−242.
(32) Gohy, J.-F.; Antoun, S.; Jerome, R. *Macromolecules* **2001**, *34*, 7435−7440.
(33) Hofs, B.; Voets, I. K.; de Keizer, A.; Cohen Stuart, M. A. *Phys. Chem. Chem. Phys.* **2006**, *8*, 4242−4251.
(34) Tanford, C. *The Hydrophobic Effect*; Wiley: New York, 1980.

MA0614444